Evaluation of Surrogate Aerosol Experiments to Predict Spreading and Removal of Virus-Laden Aerosols

Janis Beimdiek and Hans-Joachim Schmid *

Posted Date: 25 January 2024

doi: 10.20944/preprints202401.1858.v1

Keywords: surrogate aerosols; indoor air cleaners; ultra-fine particles; COVID-19; test method; field experiments: clean air delivery rate

Article

Evaluation of Surrogate Aerosol Experiments to Predict Spreading and Removal of Virus-Laden Aerosols

Janis Beimdiek and Hans-Joachim Schmid *

Particle Technology Group, Faculty of Mechanical Engineering, Paderborn University, Warburger Str. 100, 33098 Paderborn, Germany

* Correspondence: hans-joachim.schmid@upb.de; Tel.: +49-5251-60-2404

Abstract: Estimating the infection risks in indoor environments comprises the assessment of the behavior of virus-laden aerosols, i.e. spreading, mixing, removal by air purifiers etc. A promising experimental approach is based on using non-hazardous surrogate aerosols of similar size, e.g. salt particles, to mimic the virus aerosol behavior. This manuscript addresses the issue how a successful transfer of such experiments can be accomplished. Corresponding experiments in two very different environments, a large community hall and a seminar room, with optional use of air purifiers in various constellations were conducted. While high particle concentrations are advantageous in terms of avoiding influence of background aerosol concentrations, it is shown that appropriate consideration of aggregation and settling are vital to theoretically describe the experimentally determined course of particle concentrations. A corresponding model equation for a well-mixed situation is derived and the required parameters are thoroughly determined in separate experiments independently. It is demonstrated that clean air delivery rates (CADR) of air purifiers determined with this approach may differ substantially from common approaches not explicitly taking into account aggregation.

Keywords: surrogate aerosols; indoor air cleaners; ultra-fine particles; COVID-19; test method; field experiments: clean air delivery rate

1. Introduction

Starting in late 2019, SARS-CoV-2 emerged in Wuhan and spread rapidly around the globe. The rapid transmission in combination with a long period of incubation led to a pandemic of unknown extent in the modern world. Consequently, an instant demand on intensive research about the virus itself and its transmission arose to contain the pandemic. Four years later, a variety of studies and publications have led to an extended understanding and the pandemic has been overcome.

The virus SARS-CoV-2 shows pleomorphism and its size covers a range of 60 to 140 nm [1], whereby the specification of size is also dependent on the used equivalence diameter (e.g. mobility diameter, outer geometrical diameter w/o spike proteins etc.). However, SARS-CoV-2 viruses are typically assumed to be spherical and in the size range of 90-100 nm [2]. Such viruses are emitted by infected persons via different emission mechanisms such as coughing or sneezing, but also by speaking and even calmly breathing [3]. However, the virus is not emitted individually. It is embedded in saliva droplets covering several orders of magnitude in size ranging from 200 nm to several hundred microns depending on the emission mechanism [4–10]. Big droplets (> 10 µm) sediment fast. Therefore, they are typically not relevant for aerosol spreading of virus-laden particles. Smaller droplets, however, evaporate fast since ambient air is typically not saturated. This is typically happening within seconds as Xie et al. showed [11]. They shrink to small, solidified saliva residue particles of mainly submicron size. In this size range, the particles remain in the ambient air for a long period of time, typically several hours, and can accumulate in enclosed spaces [12,13]. So, even if an infectious person leaves an enclosed space, the virus-laden aerosol depicts a transmission risk by inhalation of non-infected persons [14]. In the early days of pandemic, it was assumed that, as with many other pathogens, direct contact would be the main transmission path. However, it showed that

 doi:10.20944/preprints202401.1858.v1

indirect contact by inhalation of aerosolized virus-laden particles is the main transmission path [15–17], which has also been officially recognized by the World Health Organization (WHO) [18]. For this reason, it is of utmost importance to fundamentally understand the spreading of respiratory aerosols in enclosed spaces to derive useful mitigation measures.

Investigating an aerosol consisting of the actual atomized pathogen would constitute a major health risk to researchers and would require very high safety standards. Because this is unrealizable for most academic research, alternative paths of investigation are utilized and there are mainly two approaches: using submicron surrogate aerosols or tracking a tracer gas concentration, e.g. carbon dioxide (CO_2), to mimic the spreading behavior of respiratory aerosols containing the pathogenic virus. In fact, there are two fundamentally different methods using CO_2 to assess air quality: On the one hand, CO_2 is used routinely as marker for indoor air quality, often used for the design of heating, ventilation and air conditioning (HVAC) systems. Here, CO_2 is used as indicator for the quality of air exchange observing natural exhalation of persons present in the room. Monitoring the indoor CO_2 concentration in context with SARS-CoV-2 has been carried out in various settings, e.g. theatres [19], buses [20], hospitals [21], and classrooms [22–25]. That this approach is helpful has been shown by e.g. Di Gilio et al. who derived an effective air exchange strategy in classrooms by real-time visualization and monitoring of CO_2 concentrations [25]. Rudnick and Milton used a Wells-Riley model to derive a CO_2-based risk equation for transmission of airborne pathogens [26]. Peng and Jimenez extended and adjusted the Rudnick-Milton model to SARS-CoV-2 [27]. However, tracking CO_2 concentrations for the assessment of virus aerosol concentrations has its limitations. The CO_2 concentration is proportional to the number of the present persons. However, typically there might be only one infected person in the room who is sufficient to infect others. Furthermore, air filtration, sedimentation and pathogen deactivation do not affect CO_2 levels but have an influence on the transmission risk. Bazant et al. claim to have set up a model to cover these effects for a CO_2-based description of pathogen transmission risk [28]. On the other hand, an artificial CO_2 source might be deployed in order to use CO_2 as a tracer to track its room spreading, as e.g. done by Schade et al. [29]. However, due to the quite high CO_2 background level of around 400 ppm requires rather high amounts of CO_2 to achieve reasonable accuracy. Therefore, this method is either limited to rather small rooms or to predict the spreading of viruses close to the related source.

Alternatively, aerosol spreading and removal can be examined by measuring surrogate particle concentrations directly. There are several possibilities to remove particulate matter from the ambient air by either natural ventilation or artificial means, i.e. HVAC systems or air purifiers (APs). Many studies and discussions deal with the question of the effectiveness of ventilation in comparison to air purification. Air exchange by ventilation is always needed in populated enclosed spaces to limit CO_2 concentrations. The aforementioned studies observing CO_2 concentrations emitted by persons in enclosed spaces show that concentration levels rapidly exceed values of 1000-2000 ppm, which strongly decreases mindfulness and concentration. Therefore, natural or artificial ventilation systems are definitely needed, also reducing potentially present airborne pathogens. However, air purification is an effective additional measure to further reduce transmission risks. Because installing HVAC units in enclosed spaces or modifying complete ventilation systems is labor- and cost-intensive, the pandemic created a high demand for portable APs to minimize aerosol accumulation and transmission. The quantity of purified air is called the Clean Air Delivery Rate (CADR). It describes the imaginary volume of completely cleaned air per time, i.e. the volume flow rate through the AP times the separation efficiency. If HEPA 13 filters are applied in air purifiers which have a filtration efficiency close to 100 %, filtered and cleaned air flow rates are almost identical. Another common term is the Air Exchange Rate (AER) or Air Changes Per Hour (ACH) which denotes the number of times the whole volume of air in a room gets replaced per time. In case an AP is used, particles are removed at the CADR but in effect no air is exchanged at all. Therefore, in this case it would be more precise to speak of an air purification rate when the air exchange is solely caused by an air purifier. Nevertheless, the AER / ACH is commonly used in these cases as well.

Experimental results prove the effectiveness of these devices for limiting particle concentrations [30–35]. Kähler et al. found that a stand-alone AP should be placed in the center of a

 doi:10.20944/preprints202401.1858.v1

room while multiple APs should be evenly distributed [36]. Still, if this is not feasible, Küpper et al. showed that placing APs in the corner of a room is still effective if there is no disturbance for the air flow at the intake and outlet [37]. Aerosol spreading was also described numerically to spatially resolve aerosol spreading, i.e. for a more precise evaluation of room mixing, prediction of infection risk or optimized positioning of filtering devices [38–43]. Most of these considerations mainly cover unsteady situations. If people stay in enclosed spaces long enough, they will face a steady-state concentration of aerosol particles under the assumption that the source of particles and the CADR of APs are constant. Under the condition of ideal mixing, such stationary concentrations can be calculated analytically. A facile approach is to use a simple analytic model comprising the assumption of having only two relevant influences on particle concentration within enclosed spaces: a particle source and an air purifier as particle sink [44]. Conducting experiments with surrogate aerosols typically involves high concentrations of several thousands of particles per cm^3 to describe and observe how they spread, while the realistic concentration of respiratory particles in enclosed spaces is only a few tens or hundreds of particles per cm^3. This is necessary to have a contrast to the background aerosol concentration from the environment. When deploying such high particle concentrations, some additional pathogen sinks like sedimentation or aggregation might become relevant. Therefore, evaluating experimental results from surrogate aerosols with the above-mentioned simple model, i.e. neglecting sedimentation and agglomeration, might lead to an underestimation of infection risks. This is why, commonly, a natural decay rate is considered, which means that the decline in particle concentration without an operating AP is measured as reference. This rate is then subtracted from the overall decay rate measured with an operating AP. Using such a generalized first-order loss term is well described in literature [37,44–47] and common procedure for measuring CADRs according to norms such as ANSI/AHAM AC-1-2020 [48] or GB/T 18801-2015 [49]. Further more-sophisticated models exist as well, but depict incremental models distinguishing between different concentration segments that are fitted individually [50,51] or have not been applied for data analysis of surrogate aerosol experiments [52–54]. Schumacher et al. e.g. reflected on further particle sinks for spreading of virus aerosols and estimated reduction rates for leakage flows, particle deposition and virus inactivation [55] for a theoretical model of virus aerosol spreading. They state that aggregation is of negligible relevance for those aerosols, which holds true for typical virus aerosol concentrations. However, to transfer implications from measurements with surrogate aerosols of high concentrations to virus aerosols this hypothesis is to be evaluated further and will be a major part of this work.

Within the scope of this work, investigations on particle concentration profiles and steady state concentrations by surrogate aerosols were carried out in two enclosed spaces, namely a community hall and a seminar room. As a major part of this work, the influence of high particle concentrations on the representativity of analytic models is discussed. For this purpose, the adequacy of the above-mentioned simple model is addressed followed by a discussion of the influence of additional mechanisms. Finally, a more sophisticated and extended analytic model is set up and compared to both, experimental data and the simple model. Furthermore, the transferability of the additional experimentally determined parameters in both rooms is discussed.

2. Materials and Methods

Aerosol generation

For the generation of particles, the atomizer AGK 2000 by Palas GmbH was used. It atomizes an aqueous salt solution producing initially small droplets which dry similarly fast as respiratory aerosols resulting in ultrafine solid salt particles in good representation of the particle size distribution of respiratory aerosols (size range: 20-500 nm; mean size: 100 nm; distribution provided in Supplementary Material). The atomizer was operated at a pressure of 4 bar. The necessary pressure was provided by a mobile compressor. As material for the surrogate aerosol, sodium chloride (NaCl) was chosen. A solution containing 5 wt.% NaCl was fed to the atomizer by the KD Scientific Gemini 88 Plus Dual Rate Syringe Pump at a constant rate of 1 ml/min. The pump was operating in

 doi:10.20944/preprints202401.1858.v1

reciprocating condition combined with the valve box "Medium Pressure (100 psi)" by KD Scientific for continuous liquid feed delivery.

Aerosol removal

The model Mi 3H manufactured by Beijing Smartmi Electronic Technology Co., Ltd. was chosen as air purifier. It exhibits a specified CADR of 380 m^3/h, a HEPA class 13 filter and 3 fan stages (1: low, 2: mid, 3: high flow) without specification on CADR of stage 1 and 2.

Aerosol characterization

The aerosol number concentrations were measured with different Condensation Particle Counter (CPC) models of TSI Incorporated. Two Model 3775 CPCs, one TSI Model 3752 CPC and the TSI Model 3756 UCPC were utilized in low flow mode at 0,3 l/min. According to TSI Incorporated, the D_{50} cut-off diameter is 2.5 nm for the 3756 and 4 nm for the other models. Furthermore, for determination of particle size distributions, an SMPS system combining the 3775 models with a TSI 3081 Long DMA was utilized with a sheath flow of 3 l/min and a voltage range of 10 – 10,000 V.

CPC concentration normalization

Since the four CPCs have different counting efficiencies and the UCPC even a smaller cutoff diameter, an additional measurement was conducted to determine a normalization factor for every CPC. For this purpose, a NaCl aerosol was prepared at a particle concentration below 50,000 particles per cm^3 (also the maximum applied concentration in the experiments) to assure the CPCs are measuring in single particle counting mode. Then, particle concentrations were measured with all four devices simultaneously for three hours. The acquired data were averaged to obtain a mean particle concentration measured by every CPC.

Room setups

Surrogate aerosol experiments were conducted in two different enclosed spaces. First, a large community hall with a net volume of about 2450 m^3 was examined. The setup and a cross-section of the community hall as well as the experimental installations is illustrated in Figure 1.

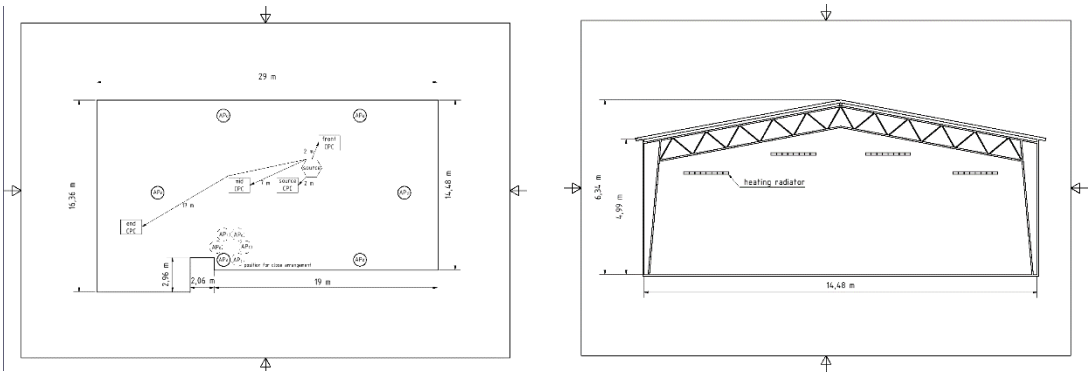

(a) (b)

Figure 1. (a) Community hall setup with positions of aerosol source, APs (in two alternative configurations) and CPCs, (b) vertical cross-section of the community hall with marked ceiling heating radiators.

As contrast to the large community hall, a small seminar room with a ceiling height of 3 m and a net volume of about 100 m^3 at Paderborn University was chosen for experimental evaluation. The related setup is depicted in Figure 2.

Preprints.org (www.preprints.org) | NOT PEER-REVIEWED | Posted: 25 January 2024 doi:10.20944/preprints202401.1858.v1

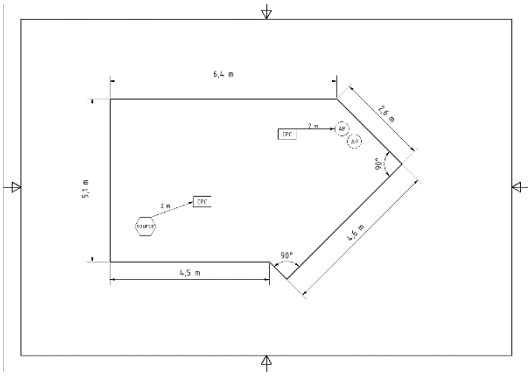

Figure 2. Seminar room setup with positions of aerosol source, APs and CPCs.

For better imagination, photos of both setups are included in the Supplementary Material.

Aerosol source strength

Prior to the surrogate aerosol experiments, the source strength of the aerosol generator was determined in a lab setup. The described surrogate NaCl aerosol was fed into a tube and diluted with a filtered compressed air flow of 200 l/min. The AGK 2000 emits a strongly fluctuating aerosol concentration. For this reason, the diluted aerosol was fed into a box equipped with four computer fans which balance the aerosol concentration. The used box has a volume of 80 L. So, the residence time in the box is less than half a minute and possible aggregation in the box can be neglected. The concentration of the resulting aerosol is then measured simultaneously by the two 3775 CPC models.

Surrogate aerosol experiments

Several experiments in both locations were conducted in order to compare the experimentally determined, time dependent evolution of the particle concentration to different models (cf. Table 1). Prior to every experiment, all APs were running for a sufficiently long time (e.g. overnight in case of community hall) until a constant background aerosol concentration (typically less than 500 particles per cm^3) was achieved. A further reduction was not possible, indicating some remaining natural particle sources, like plants, leakage flows from outside etc.).

Table 1. List of conducted experiments comprising their acronym, location, AP settings and main purpose.

Acronym	Location	Number of used APs	Applied fan stage	Arrangement of APs	Purpose
C_maxAP_d	Community Hall	6	3	Distributed	Model comparison
C_minAP_d		6	1	Distributed	Model comparison
C_maxAP_c		6	3	Close	Model comparison
C_noAP		0	-	-	Model comparison
S_maxAP	Seminar Room	2	3	Close	Model comparison
S_noAP		0	-	-	Model comparison
S_fit_lowc S_fit_midc S_fit_highc		0	-	-	fit of model parameters

 doi:10.20944/preprints202401.1858.v1

When air purifiers were used in the experiments for a comparison with analytic models, they were running continuously during the complete experiment. This includes measuring the decline in concentration when the particle source was turned off. These data were evaluated for CADR determination as well.

The S_fit experiments mentioned in Table 1 were conducted to estimate kinetic coefficients for sedimentation and aggregation as additional parameters to be included in an extended analytic model. Therefore, the decline of concentration from three different start concentrations of approx. 10,000 (lowc), 20,000 (midc) and 30,000 (highc) particles per cm^3 was measured. The different start concentrations were chosen to evaluate the impact of a potential change in the decline rate depending on the change in particle size distribution caused by aggregation. In order to start from a balanced room concentration in these three measurements, two ventilators were operated for 5 minutes when the particle source was turned off. Additionally, SMPS measurements were conducted periodically to track the evolution of particle size distribution.

3. Results

3.1. Evaluation of mixing quality in the examined spaces

Before comparing the measured concentration profiles to analytic considerations, the question of mixing and homogeneity of spatial particle distribution within the examined locations needs to be addressed. In Figure 3, the experimental results obtained in the community hall without application of air purifiers are illustrated and various observations can be made.

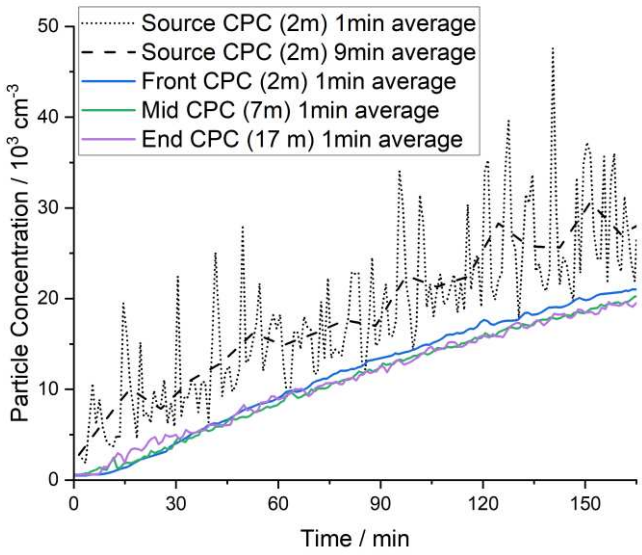

Figure 3. Concentration profiles for experiment C_noAP (community hall without APs, measured at different locations according to Figure 1).

First, it takes a few minutes until an increase of particle concentration is detected by the 'Front' (distance of 2 m to particle source), "Mid" (distance of 7 m) and "End" (distance of 17 m) CPC. In the first minutes of the experiment, the measured particle concentrations from the three CPCs differ slightly since there is no instant mixing. However, after 30 minutes at latest, the particle concentration of the 'Mid' and 'End' CPC matches the concentration of the 'Front CPC' with minor, mainly statistical differences. Surprisingly, the End CPC detects particles already shortly after starting the experiment and on top of that it detects a rise in concentration before the Front CPC although the distance to the particle source is 17 m compared to 2 m for the Front CPC. This enormous fast response of the End CPC combined with a non-significant difference to the measured concentration profiles at other measurement positions, must be attributed to very excellent mixing in the

 doi:10.20944/preprints202401.1858.v1

community hall. At the ceiling of the hall, heating radiators are installed (cf. hall cross-section in Figure 1). Since the experiments were carried out in December at a few degrees Celsius outdoor temperature, these radiators were running. In addition, the roof is not isolated very well, which has apparently resulted in a significant temperature gradient. It is evident, that these particular conditions provided an extensive convective flow circulation and thus good mixing could unexpectedly be achieved within relatively short times even at large distances. Furthermore, this might be an explanation why the End CPC detects additional particles before the Front CPC which might be caused by the vertically directed, circular flow. Overall, this illustrates that the mixing within the community hall can be considered ideal in good approximation when looking at long-term trends.

Second, the particle counter 'Source CPC' (cf. Figure 1a), also in a proximity of 2 m to the particle source, shows a significant difference in measured particle concentrations. As already mentioned in the experimental section, a compressor was used to generate the pressure needed for the atomizer. When the compressor was running, it appeared that additional particles were generated. Whereas the salt aerosol is emitted in vertical direction and therefore immediately distributed to the environment, the particles generated by the compressor were obviously entrained in a directed exhaust air flow and emitted in a specific direction towards the 'Source CPC'. This causes the strong fluctuations in the corresponding concentration profile (corresponding to an operation interval around 5-6 minutes for the compressor), which is still clearly visible, although data is averaged in a one-minute interval. It is possible that there is also some directed macroscopic flow from the natural convection inside the hall, which would further explain why the 'Mid' and 'End' CPC show a rise in particle concentration slightly before the 'Front' CPC which is located in opposite direction of the particle source. To smoothen the concentration profile of the 'Source CPC' for a comparison to the other concentration profiles, a nine-minute averaging time was chosen for this device. Although generating additional particles by the compressor was an unintended effect, it mimics to a certain extent the real case of respiratory aerosol particle emission which has a specific direction as well. The 'Source' CPC located directly in the particle stream from the compressor at 2 m distance measures an average particle concentration which is approx. 1.5 to 2-times higher than the mean concentration in the room. However, the 'Front' CPC, also at a distance of 2 m from the particle source but in opposite direction to the particle stream from the compressor shows almost mean room concentration. This implies that the direction of particle emission might be more significant than the exact distance to the particle source. Even at a distance of 2 m, which is often considered as 'Safe Distance', the concentration might be 1.5 to 2-times higher, if there is a directional transport of the aerosol, as it is typical for exhaled particles. In proximity to the particle source, the assumption of ideally mixed and homogeneously distributed particles in the room no longer applies. Referring this to virus-laden aerosols, persons close to a virus-emitting person breathe a higher concentration of harmful viruses when they stand in direction of the exhalation flow. However, the observed additional particle generation by the compressor with a directional transport can be seen as worst-case scenario.

In case of the seminar room, ideal mixing could not be proven. Due to the small distances in the room and the classical heat radiators located below the windows, the spikes in the particle concentration profiles caused by the compressor are still visible to some extent even in the measured concentrations close to the two air purifiers in the opposite corner of the room (cf. Figure 2), which might be due to the directed exhaust stream of the compressor.

 doi:10.20944/preprints202401.1858.v1

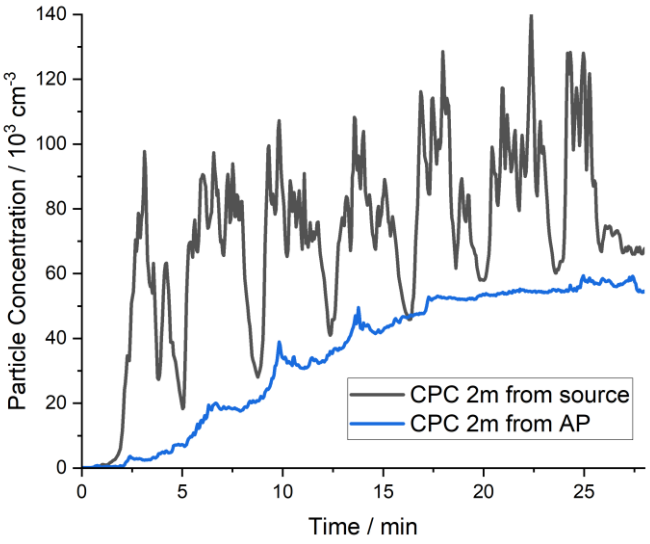

Figure 4. Measured concentration profiles of experiment S_noAP (seminar room, air purifiers out of operation).

Since the assumption of ideally mixed air is more reasonable in the community hall, most of the following considerations discussed are related to those experiments, while the decay experiments in the seminar room with a short ventilation phase after shutting down the particle source are examined for a closer look on sedimentation and aggregation.

3.2. Influence of air purifier power and and arrangement on concentration profiles

For the experiments with applied air purifiers in the community hall, the previously shown effect of almost ideal mixing is observed as well. For this reason, only one representative curve averaged from the three similar concentration profiles is shown in the following considerations. In Figure 5, the experimental results for evenly distributed air purifiers at maximum power is compared to the case of distributed air purifiers at minimum power and to the case of air purifiers at maximum power in a close arrangement in one place (cf. Figure 1a).

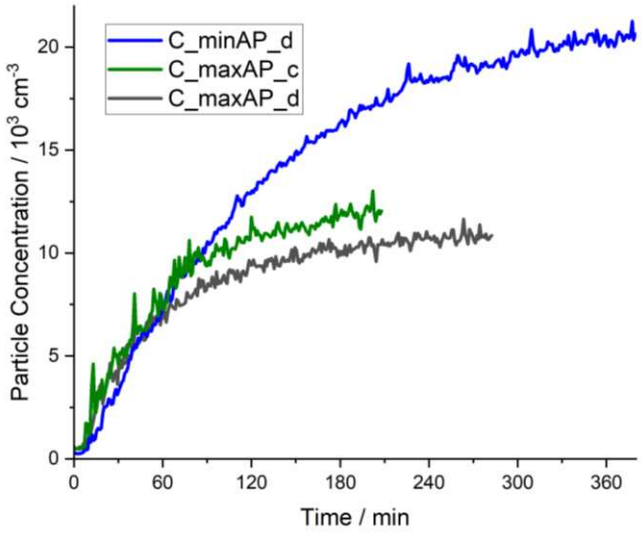

Figure 5. Concentration profiles of experiments with operating air purifiers in different configurations at the community hall: APs distributed and operated at level 1 (C_minAP_d); APs arranged close and operated at level 3 (C_maxAP_c); APs distributed and at level 3 (C_maxAP_d).

 doi:10.20944/preprints202401.1858.v1

Comparing the influence of distribution of air purifiers, the scenario of distributed air purifiers yields a steady state concentration of approx. 10,500 particles per cm^3, while a close arrangement of air purifiers in one corner of the hall exhibits a stationary concentration of around 12,000 particles per cm^3. This is an expected effect: The short distance between the closely arranged air purifiers enables bypass flows, i.e. air purifiers draw in already cleaned air, which results in a reduced effective CADR and consequently a higher stationary concentration. Furthermore, a reduction of fan power from level 3 to level 1 almost doubles the stationary concentration which then amounts to 20,500 particles per cm^3.

3.3. Model-based evaluation of surrogate aerosol experiments

3.3.1. Simple analytic modelling of surrogate aerosol experiments

When trying to assess the effectiveness of air purifiers (AP) or other measures to reduce aerosol concentrations by surrogate aerosols, experimental results are often compared to a simple model described by two terms assuming ideal mixing: the particle generator as source term $\dot{S}$ and the CADR $\dot{V}_{CADR}$ as sink term if an air purifier is used. This case can be described mathematically with the differential equation:

$$V \cdot \frac{dc}{dt} = -\dot{V}_{CADR} \cdot c + \dot{S} \tag{1}$$

where c denotes the concentration, t the time and V the room volume.

Introducing a characteristic time τ:

$$\tau = \frac{V}{\dot{V}_{CADR}} \tag{2}$$

where τ can be interpreted as the air purification time, i.e., the time theoretically needed for cleaning the room air once completely, if no mixing would apply.

Using this equation (2) and the assumption of c(t = 0)=0, equation (1) can be solved to:

$$c(t) = \frac{\dot{S}}{\dot{V}_{CADR}}\left(1 - e^{-\frac{t}{\tau}}\right) = c^* \cdot \left(1 - e^{-\frac{t}{\tau}}\right) \tag{3}$$

with the steady state concentration c^*. Counter-intuitively, the room volume has no influence on this c^*. As small as the air purifier is, it will yield the same c^* in a small seminar room as in a big community hall as long as ideal mixing is assured and other particle losses are negligible. The volume only influences the time to achieve the steady state. The steady state concentration, however, is solely dependent on source strength and particle removal rate, namely CADR. This also implies that c^* is independent of the AER. Consequently, the common recommendation during the COVID-19 pandemic that in order to achieve an efficient reduction of infection risk by air purifiers requires an air exchange rate between 5 h^{-1} and 10 h^{-1}, is not supported in terms of stationary concentrations. If the indoor air is ideally mixed, the CADR can therefore not be derived by the common AER recommendation and needs to be evaluated individually for every case to keep aerosol concentrations below a certain value.

As explained before, the experimental results of this work show that the prerequisite of ideally mixed air is fulfilled in good approximation, which enables a reliable comparison to the simple model, which is shown in Figure 6.

 doi:10.20944/preprints202401.1858.v1

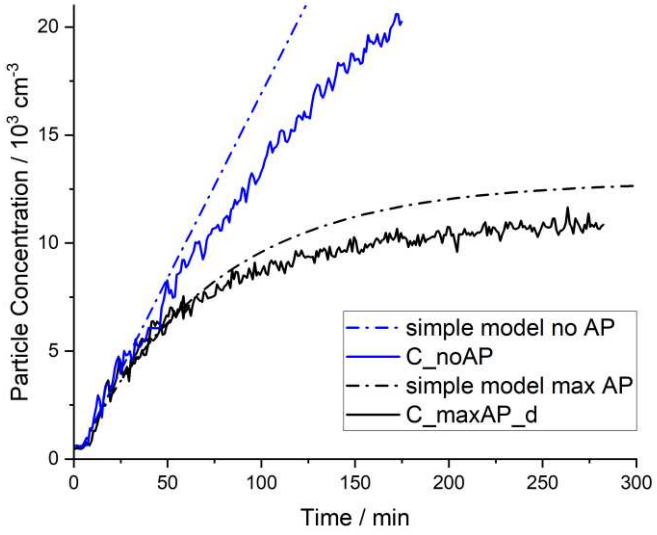

Figure 6. Comparison of experimental data to the predicted values by the simple model for the scenarios in the community hall with air purifiers running at highest level (C_maxAP_d) and shutted down (C_noAP), respectively.

Comparing the experimental data to the simple model, the observation can be made that starting at a concentration of around 5,000 particles per cm³ the simple model deviates progressively with increasing concentration. Note that for the simple model with applied air purifiers, a value of 340 $\frac{m^3}{h}$ for the CADR was used as determined and explained later in this article. In this case the same conclusion is substantiated, that particle sinks other than the CADR become relevant above particle concentrations of 5,000 particles per cm³. Natural ventilation through leakage flows, deposition of particles at surfaces, aggregation, or sedimentation of particles depict further particle sinks and their implementation into the mathematical model will be discussed in the following chapter 3.3.2.

3.3.2. Extended analytic modelling of surrogate aerosol experiments

The above-mentioned phenomena of additional particle sinks can be divided into two categories. Losses due to deposition of particles at surfaces and sedimentation are proportional to the particle concentration. Natural ventilation is depending on the difference to the environmental aerosol concentration. However, since indoor surrogate aerosol concentrations are typically one or two orders of magnitude larger than outdoor concentrations this loss mechanisms can be considered with good approximation as proportional to the concentration as well. All these phenomena are considered in a kinetic coefficient k_s which will be referred to as sedimentation coefficient throughout this work because sedimentation is believed to be the dominant mechanism in most cases. However, it should always be kept in mind, that this 'sedimentation' coefficient also reflects the above mentioned phenomena as well. The second category is determined by aggregation which is proportional to the squared concentration and considered by the kinetic coefficient k_a.

Considering these two coefficients, the ordinary differential equation (ODE) for theoretical description of particle concentration with surrogate aerosols in a well-mixed situation reads as:

$$V \cdot \frac{dc}{dt} = -(S \cdot k_s \cdot c + V \cdot k_a \cdot c^2) - \dot{V}_{CADR} \cdot c + \dot{S} \qquad (4)$$

with S denoting the room's horizontal deposition surfaces such as tables, installations and the floor area. However, for diffusional deposition which is also included in k_s, vertical walls have to be considered as well. Therefore, S rather reflects a weighted mix of surfaces, being equal to the horizontal surfaces only, when sedimentation is truly the dominating linear loss mechanism.

 doi:10.20944/preprints202401.1858.v1

Therefore, all loss mechanisms which are linearly (or approximately linear as in the case of leakage flows) proportional to the actual concentration are summarized in one loss factor k_l^* which is room specific since it contains different surfaces and the room volume:

$$k_l^* = \frac{S k_s}{V} \tag{5}$$

The first step to solve this equation is the separation of variables:

$$\int_{c_0}^{c(t)} \frac{dc}{k_a c^2 + \left(\frac{\dot{V}_{CADR}}{V} + k_l^*\right) c - \frac{\dot{S}}{V}} = -\int_0^t dt \tag{6}$$

Integrating both sides of the equation leads to:

$$\frac{2ac + b - \sqrt{D}}{2ac + b + \sqrt{D}} = E e^{-\sqrt{D}t} \tag{7}$$

In equation (7), the parameters a, b and D were introduced to get a readable representation of the solution of the ODE. The three parameters are given as:

$$a = k_a \tag{8}$$

$$b = \left(\frac{\dot{V}_{CADR}}{V} + k_l^*\right) \tag{9}$$

$$D = 4k_a \frac{\dot{S}}{V} + \left(\frac{\dot{V}_{CADR}}{V} + k_l^*\right)^2 = 4a \frac{\dot{S}}{V} + b^2 \quad \text{with } D > 0 \tag{10}$$

The integration constant E is determined using the initial condition $c(t = 0) = c_0$:

$$E = \frac{2ac_0 + b - \sqrt{D}}{2ac_0 + b + \sqrt{D}} \tag{11}$$

Transposing equation (11) finally leads to the equation which can be used to calculate the evolution of particle concentration:

$$c(t) = \frac{\left(b + \sqrt{D}\right) E e^{-\sqrt{D}t} - b + \sqrt{D}}{2a\left(1 - E e^{-\sqrt{D}t}\right)} \tag{12}$$

A direct fit of the parameters defined in equations (8) to (10) to experimental data would easily allow to get a good agreement between model and experimental data. However, we conducted separate experiments with the aim to determine the involved parameters individually based on physical reasoning. The respective approaches to determine these parameters are shown in the following sections.

3.3.3. Determination of particle generation rate

The measured generated particle concentration was $2 \cdot 10^6$ particles per cm³ in a lab setup as described in section 2. The particle concentration was obtained after dilution of the aerosol by an additional air gas flow of 200 l/min. Multiplying both values, a mean particle generation rate of $7 \cdot 10^9$ particles per second is calculated. To estimate the additional number of particles from the compressor, the particle generation was evaluated with filtering the outlet air of the compressor and without operation of the aerosol generator. Furthermore, the compressor was operated continuously instead of periodic as in the experiments to get an upper limit estimate for the particle generation rate caused by the compressor. The concentration profile of this test (corrected by the background concentration) in comparison to the experiment in the seminar room with air purifiers switched off (S_noAP) is shown in Figure 7. As can be seen, the source strength of the compressor is orders of magnitude smaller than the salt surrogate aerosol source used.

 doi:10.20944/preprints202401.1858.v1

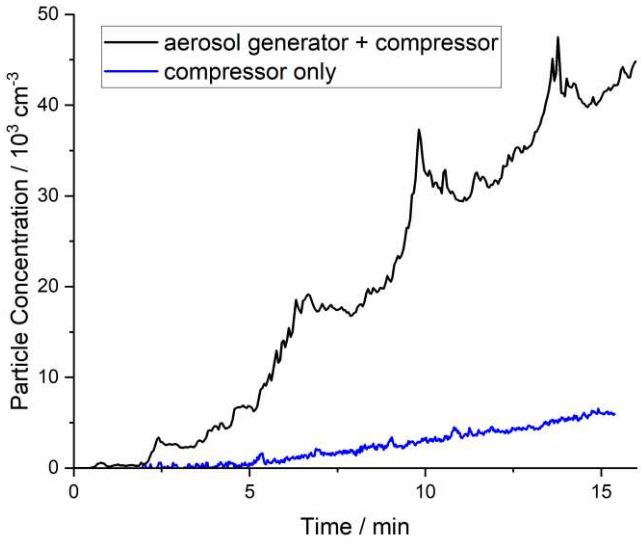

Figure 7. Comparison of the increase in room concentration for experiment S_noAP and the pure particle generation by the compressor at continuous operation.

This might appear surprising, looking at the spikes which were detected for all experiments in proximity to the aerosol source. However, these spikes result from two different reasons: Firstly, a directed flow of exhaust gas contaminated with particles contributes to these spikes, although the average total strength of this source is quite small as shown above. Secondly, a significant amount of particles from the compressor is contained in the air flow used to atomize the salt solution. This type of particle source from the compressor is not detected in the experiments in Figure 7 when the compressor air flow is filtered as it is the case in the experiment with the compressor only. During standard experiments and while determining the aerosol source strength, this flow is not filtered and consequently these additionally generated particles will result in a periodic fluctuation of the aerosol source concentrations leading to corresponding fluctuations in room concentration in the vicinity of the aerosol source. However, this type of additional particles has already been included when determining the average source strength as described above. So, the comparison reveals that the number of particles generated by the compressor which were not included in the measured source strength is minor at a rate of 500 particles per cm³. Therefore, these additional particles are neglected, and the source strength is set to the above determined particle generation rate of $\dot{S} = 7 \cdot 10^9$ particles per second.

3.3.4. Consideration of sedimentation and aggregation

A major part of this work aims to quantify the relevance of sedimentation and aggregation on obtained results. For this purpose, the kinetic coefficients k_s and k_a were determined experimentally by a fit to the three decay experiments S_fit in the seminar room. For this fit, the ODE in equation (4) can be simplified by setting the source strength $\dot{S}$ and the CADR $\dot{V}_{CADR}$ to zero. The parameters defined in equation (8) to (10) then read

$$a = k_a \tag{13}$$

$$b = k_l^* \tag{14}$$

$$D = k_l^{*2} \tag{15}$$

Integrating these parameters into equation (12), the concentration function simplifies to:

Preprints.org (www.preprints.org) | NOT PEER-REVIEWED | Posted: 25 January 2024 doi:10.20944/preprints202401.1858.v1

$$\frac{c(t)}{c_0} = \frac{\Pi_{s,0}}{(1+\Pi_{s,0})e^{k_l^* t} - 1} \tag{16}$$

with the dimensionless ratio $\Pi_{s,0}$ which is given by:

$$\Pi_{s,0} = \frac{k_l^*}{k_a c_0} \tag{17}$$

The analyzed decay data are presented in Figure 8. It shows that the data of all three experiments – each one of a 'freshly' produced aerosol with initial concentrations of 10,000 cm^{-3}, 20,000 cm^{-3}, and 30,000 cm^{-3}, respectively – combine to one graph very well. This means that particle size changes due to aggregation do not modify the aggregation kinetics significantly and constant k_a can be assumed under these conditions. Note that the gaps between data points are caused by the periodically conducted SMPS measurements.

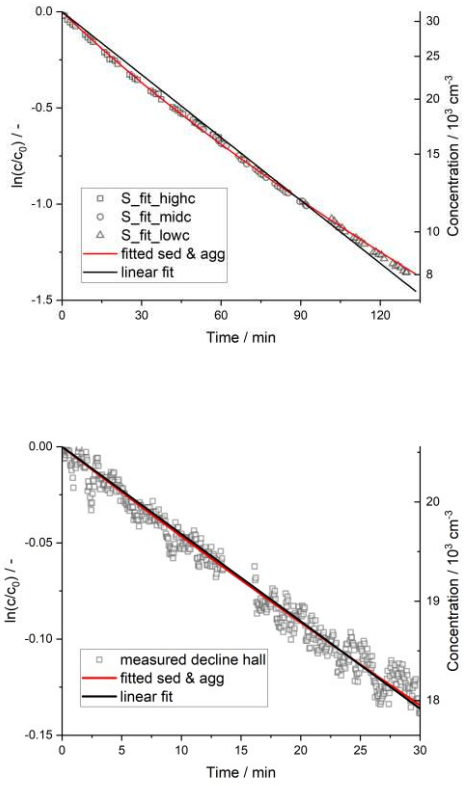

Figure 8. Fitted experimental data for determination of kinetic parameters for sedimentation and aggregation in the seminar room (left) and in the community hall (right); $k_a = 3.46 \cdot 10^{-9} \frac{cm^3}{s}$; k_l^* fitted individually.

The fit of experimental data to equation (16) results in the values $k_l^* = 1.14 \cdot 10^{-4} \frac{1}{s}$ and $k_a = 3.46 \cdot 10^{-9} \frac{cm^3}{s}$ for the seminar room. In the community hall, similar experiments were carried out but only for a limited time of 30 min. The corresponding fit of equation (16) results in $k_a = 3.9 \cdot 10^{-9} \frac{cm^3}{s}$ which is in reasonable agreement with the estimation for the seminar room. Comparing both cases, the seminar room experiments cover a much broader range of concentrations for fitting the decline in concentration. Therefore, the determined value for k_a in the seminar room is believed to be more accurate. Consequently, this value for k_a was fixed for both cases, which results in a value of $k_l^* = 1.0 \cdot 10^{-5} \frac{1}{s}$ for the community hall. As can be seen from Figure 8, the resulting fit describes the course of the measured concentrations very well. The data scatter for the community hall appears significantly larger than in the seminar room since the scale is much larger in this case.

 doi:10.20944/preprints202401.1858.v1

For comparison, a linear fit of the concentrations is shown in Figure 8 for the respective cases as well. However, a linear fit would be obtained only, if the decay is linearly proportional to the concentration as for sedimentation, wall deposition, natural convection etc. The apparent curvature in the measured concentration profile clearly shows that non-linear particle sinks exist. A second-order loss term must be considered to represent this curvature, which leads to the conclusion that aggregation which is proportional to the concentration squared is a loss mechanism which cannot be neglected at such high particle concentrations.

The linear loss term k_l^* appears to be about a factor of 10 smaller in the community hall compared to the seminar room. In case of pure sedimentation, i.e. $k_l^* = k_s \cdot \frac{S}{V}$, S depicts the floor area and the ratio $\frac{S}{V}$ can be simplified to $\frac{1}{H}$ with H denoting the room height. Assuming pure sedimentation, the ratio of k_l^* for both rooms should be equal to the ratio of room heights, i.e. k_l^* in the seminar room should be larger by a factor of 2 due to corresponding simplified geometrical considerations. However, since no ideal, empty rooms were investigated just considering the ratio of room heights is obviously not sufficient although this cannot explain the large deviation of the expected ratio of k_l^* for both locations. It can be concluded that additional mechanisms are more relevant in the seminar room. It is likely that natural ventilation by leakage flows is the most relevant mechanism since old, wooden windows are installed in the seminar room. In general, this underlines that the room-independent kinetic constant k_s is hard to determine from isolated measurements but moreover k_l^* has to be determined for any room set-up separately by fitting concentration decay without any air purification.

The relevance of the parameters k_l^* and k_a is illustrated in Figure 9. For the experiment in the community hall with air purifiers switched off (C_noAP), the relevance of considering sedimentation and aggregation is demonstrated. The simple model would suggest a linear increase in concentration, which results in progressive deviations to experimental data at concentrations above around 5,000 particles per cm³. Considering sedimentation but no aggregation, results in a small curvature of the concentration profile while considering only aggregation but no sedimentation can represent the curvature of experimental data better but still overpredicts the concentration. Consequently, both mechanisms, sedimentation (or better: linear mechanisms) and aggregation, need to be considered to get a suitable representation of the concentration profile and neither can be neglected. This supports the hypothesis that the presented extended model in equation (11) is an adequate mathematical approach to evaluate surrogate aerosols and should be used at least beyond 5,000 particles per cm³.

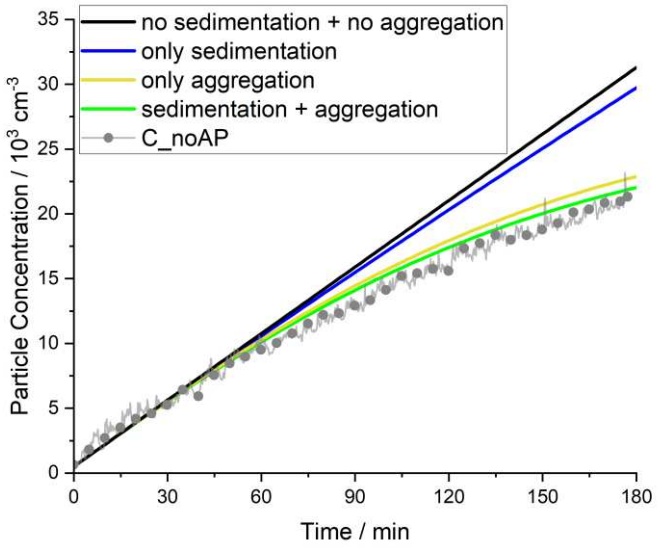

Figure 9. Influence of aggregation and sedimentation on resembling experimental data for the scenario in the community hall with APs switched off (C_noAP).

 doi:10.20944/preprints202401.1858.v1

To check for plausibility, the experimentally determined k_a is compared to theoretical considerations. For this purpose, the approach by Lee and Chen [56] is used to calculate a theoretical aggregation coefficient. For a particle size of 100 nm (mean value of the distribution in this work), the gas-slip regime must be considered. Following their calculations, the theoretical aggregation coefficient is $k_{a,theory} \approx 1 \cdot 10^{-9} \frac{cm^3}{s}$ for a geometric standard deviation of 2 as measured in the present case (see supplementary material). Comparing this simply estimated theoretical coefficient to the experimentally determined $k_a = 3.46 \cdot 10^{-9} \frac{cm^3}{s}$, the presented experimental procedure can be considered an adequate approach and the fitted k_a represents a valid value for the aggregation coefficient of the used surrogate aerosol.

3.3.5. Examination of the Clean Air Delivery Rate (CADR) of applied air purifiers

The aim of determining all relevant model parameters based on physical reasoning also includes the CADR as it determines the steady state concentration for the most part as discussed earlier. So, the CADRs of the air purifiers were determined experimentally instead of relying on the manufacturer's specification that the air purifiers exhibit a CADR of $380 \frac{m^3}{h}$. A fit of equation (12) to the respective experimental data allows the determination of the corresponding CADRs as given in Table 2. It turns out that the CADRs are significantly below the manufacturer's specification of 380 $\frac{m^3}{h}$. The measured CADRs with air purifiers arranged close to each other (S_maxAP with two and C_maxAP_c with six APs in close proximity each) reflect the effect of bypass flows (cf. section 3.2) pretty well. However, it appears that this effect is way more important in the much smaller seminar room. Particularly the ceiling height might be important here because the air purifiers blow the cleaned air vertically upwards.

To show the accuracy of the model fit, the measured concentration profiles are depicted in Figure 10 together with the results from the extended model using the respective CADRs. Comparing the different scenarios, the extended model can describe the concentration profiles of all scenarios pretty well, particularly in case of the experiments in the community hall. For the seminar room, the model slightly underestimates the concentration, however, it needs to be considered that ideal mixing was not achieved in this case as discussed before.

Table 2. Experimentally determined CADRs per air purifier by evaluation according to equation (12).

	C_maxAP_d	**C_minAP_d**	**C_maxAP_c**	**S_maxAP**
Start concentration / $\frac{1}{cm^3}$	10.000	20.000	10.000	30.000
End concentration / $\frac{1}{cm^3}$	7.000	18.000	7.000	4.000
Model fit CADR / $\frac{m^3}{h}$	340	65	330	290

Preprints.org (www.preprints.org) | NOT PEER-REVIEWED | Posted: 25 January 2024 doi:10.20944/preprints202401.1858.v1

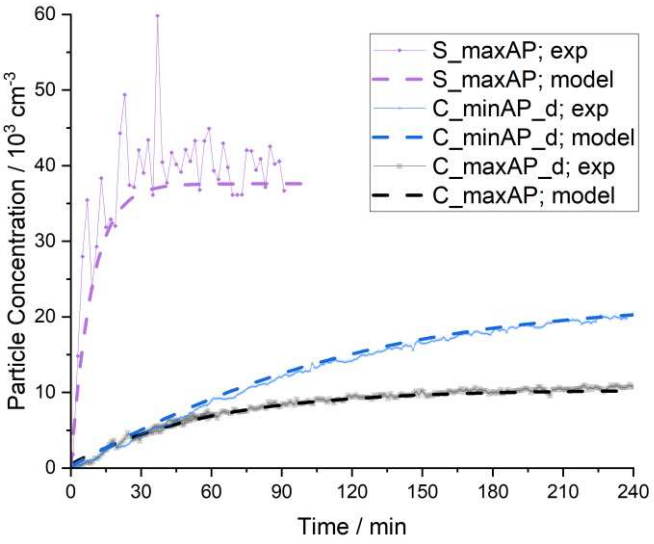

Figure 10. Comparison of measured data to the extended model with independently determined model parameters.

3.3.6. Comparison to standard procedure of CADR determination

As briefly outlined in the introduction, the determination of the CADR of air purifiers is also regulated by various norms (e.g. ANSI/AHAM AC-1-2020 from the US or GB/T 18801-2015 from China). The common practice to determine the CADR according to those norms deviates from the approach presented in this work and the following section will discuss the differences in the results of the obtained CADRs.

The standard procedure always assumes an exponential decay of concentrations with time, i.e. a linear decay of the logarithmic concentration ratios. The determination of the corresponding CADR is then obtained in two steps: First, in order to account for any additional particle losses except removal by the air purifier, a linear decay of the concentration in the case of air purifiers switched off is assumed, which is typically referred to as natural decay. Consequently, a characteristic time, namely the natural decay time τ_n, is determined by fitting the concentration decay (typically for 20 min) with air purifiers switched off:

$$c_n(t) = c_0 \cdot e^{-\frac{t}{\tau_n}} \quad \text{or} \quad ln\frac{c}{c_0} = -\frac{t}{\tau_n} \tag{18}$$

This approach has also been depicted in Figure 8 referred to as 'linear fit'.

Second, a fit of the experimental data with air purifier turned on is done in the same setup for the same time interval to obtain a characteristic decay time constant τ_{AP}:

$$c_{AP}(t) = c_0 \cdot e^{-\frac{t}{\tau_{AP}}} \quad \text{or} \quad ln\frac{c}{c_0} = -\frac{t}{\tau_{AP}} \tag{19}$$

The overall decay in case of air purifiers in operation is then assumed to be a superposition of the natural decay and the so-called effective decay, caused by the air purifiers only:

$$c_{AP}(t) = c_0 \cdot e^{-\frac{t}{\tau_{AP}}} = c_0 \cdot e^{-\left(\frac{1}{\tau_{eff}}+\frac{1}{\tau_n}\right)\cdot t} \tag{20}$$

Since any characteristic decay time can be associated with a corresponding CADR-value, one can obtain the effective CADR straightforward:

 doi:10.20944/preprints202401.1858.v1

$$CADR_{eff} = CADR_{AP} - CADR_n \qquad \text{with each} \quad CADR_i = \frac{V}{\tau_i} \tag{21}$$

However, as shown in Figure 8, the natural decay is not linear. Moreover, the effect of aggregation which is proportional to the concentration squared causes a curvature of the logarithmic concentration decay. Therefore an 'actual' natural decay rate is calculated by determination of the derivative from equation (16), as fitted to the experimental data and parameters according to section 3.3.4. As shown in Figure 11, this calculated actual decay rate strongly depends on the actual concentration. While aggregation (given by the term $k_a \cdot c^2$) is assumed to be independent of the respective room, the other, linear natural decay mechanisms (hence given by the term $k_l^* \cdot c$) may strongly depend on the respective setting. Since the value of k_l^* in the seminar room is an order of magnitude larger than in the community hall, the natural decay rate in the seminar room is also significantly larger. However, the natural decay rate $1/\tau_n$ in the seminar room is increasing about a factor of 2 for the concentration increasing to $3 \cdot 10^5 cm^{-3}$ while it is increasing by more than a factor of 10 in case of the community hall. This reflects the much larger impact in case of the community hall, since the ratio of aggregation kinetics to other decay mechanism (linearly depending on concentration) is much larger there. Furthermore, Figure 11 also shows the corresponding $CADR_n$ calculated according to equation (21). It clearly shows the much larger effect of natural decay in case of the very large volume there. This indicates that a large volume is unfavourable for determining the $CADR$ of air purifiers with high accuracy.

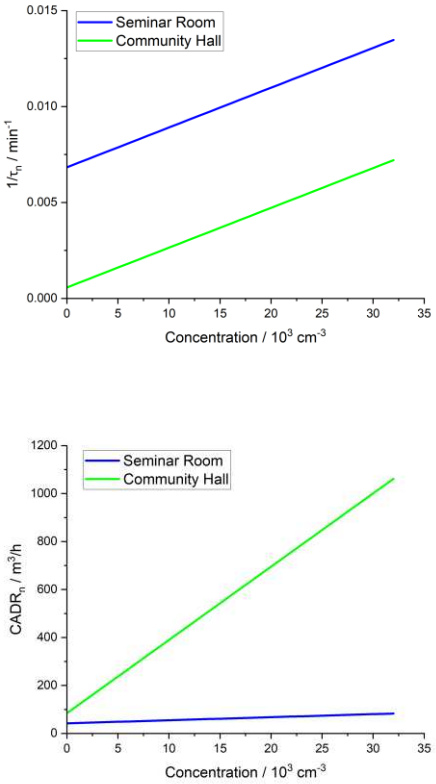

Figure 11. Natural decay in different settings (seminar room and community hall) with respect to actual concentration: natural decay rate (left) and corresponding $CADR_n$ (right).

Applying the 'standard method' to determine the CADR requires a linear fit of the logarithmic concentration decay, somehow averaging the decreasing slope due to the declining aggregation with reducing concentration. However, since typically both measurements, i.e. decay with air purifiers on and off respectively, are done for the same time, the final concentration with air purifiers switched off is significantly higher compared to the case when air purifiers are switched on. Therefore, due to

 doi:10.20944/preprints202401.1858.v1

the higher average concentration during the natural decay measurement, aggregation is stronger in this case. Therefore, a systematic overestimation of the natural $CADR_n$ and consequently a systematic underprediction of the effective $CADR_{eff}$ can be expected. Furthermore, it can be expected that this effect is even more pronounced for longer time intervals of the decay measurement.

This systematic error can be evaluated for the measurements described above: Figure 12 shows the respective concentration profiles. In order to eliminate errors due to measurement fluctuations, the fitted data instead of the actual experimental data is used here. It should be noted that the different experiments started at quite different initial concentrations and the different air exchange rates in both rooms cause a significantly differing decline in concentration. This data and the respective data from natural decay (cf. Figure 11) can be used to determine the $CADR_{eff}$ by applying equations (18),(19) and (21) for varying time intervals and alternatively using the $CADR$ from Table 2, determined by fitting equation (12), as reference. The relative deviation D is then calculated by:

$$D = \frac{CADR_{fit} - CADR_{eff}(t)}{CADR_{fit}} \tag{22}$$

This deviation is shown in Figure 12 as well. All deviations are positive, which confirms the presumption that the standard method systematically underestimates the CADR value. Comparing the deviation for the two experiments in the community hall shows that the higher concentration in the experiment with low fan level (C_minAP_d) results in significantly higher deviations. This can be explained by the larger impact of aggregation for higher particle concentrations and the fact that the deviation D is a relative deviation, i.e. for higher CADR even the same absolute error would result in a smaller relative error. The experiments in the seminar room are characterized by a very high initial concentration followed by a strong decline due to the high air exchange ratio. For short time intervals, a very high gradient in particle concentration exists which in this case leads to deviations comparable to the community hall with low fan level (C_minAP_d). However, for larger evaluation times exhibits a maximum followed by a very small decline.

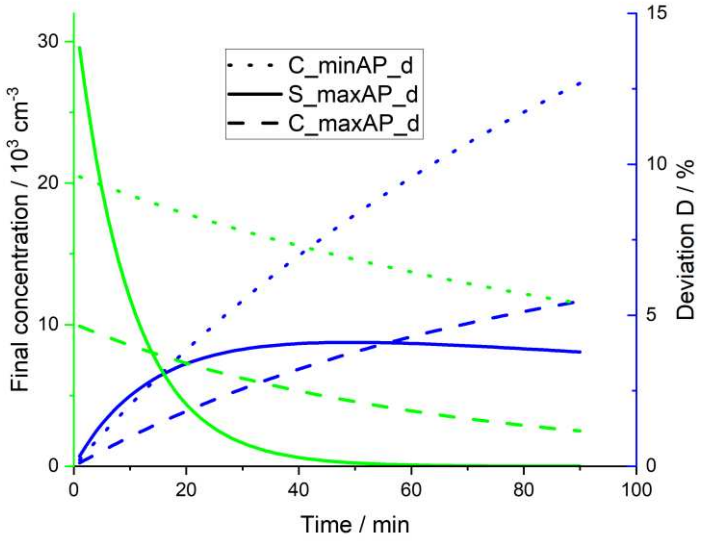

Figure 12. Time-dependent concentration (fitted) for three different cases (green) & deviation D of obtained CADR from fit to extended model (equation 12) compared to CADR determined by the 'standard procedure' with respect to the applied time interval (equations 18/19/21) (blue).

In order to better understand the influence of experimental conditions and evaluation on obtained CADR values, a systematic parameter study has been performed shown in Figure 13. Again, all deviations are positive, confirming that the discussed effect leads to a systematic underestimation of the CADR by the 'standard method'. The diagrams a-c are determined for parameters reflecting

 doi:10.20944/preprints202401.1858.v1

the situation in the seminar room, i.e. a case with rather high k_l^* with varying initial concentration c_0. It can be clearly seen, that for high air exchange rates the error is rather low, even for very high initial concentrations of $5 \cdot 10^4$ cm^{-3} the deviation never exceeds 5 %. However, for small exchange rates the relative deviation increases significantly. At first glance, this might appear counter intuitive: The steeper the gradient in concentration, i.e. high exchange rates, the stronger the effect of different aggregation kinetics for air purifiers switched on and off, respectively, will be. Consequently, the absolute deviation is larger in case of high air exchange rates. However, the deviation *D* is related to the actual CADR which obviously overcompensates the increasing deviation. Consequently, for small air exchange rates, particularly below around 2 h^{-1}, the deviation is strongly increasing for increasing evaluation time intervals and might reach values even higher than 10%. For high air exchange rates, one can observe a maximum in deviation for medium evaluation time intervals as already seen in Figure 12. This can be explained by the fact that, in these cases, concentrations become so low after some time that aggregation is not relevant at all. Therefore, concentrations during the natural decay experiments with longer evaluation times will reflect this situation better and hence the deviation is decreasing for longer time intervals.

Comparing Figure 13 a & d reveals that the difference in k_l^* does not change much in the deviation although aggregation is much more relevant compared to settling in the second case. However, if the decay due to air purifiers is stronger than the natural decay, the ratio of aggregation – which is the reason for any deviation discussed here – to air removal is more relevant.

Finally, Figure 13 e & f show the deviation with respect to initial concentration and air exchange rate for 20 min and 60 min evaluation time interval, respectively. The deviation for 20 min is below 5 % in most relevant cases since the concentration should be kept below $5 \cdot 10^5$ cm^{-3} because this is the limit for the CPC to operate in counting mode. Although 20 min is the standard time interval proposed in the norms, for evaluation of aerosol dynamics in a room quite longer times might be of interest. Therefore, diagram f shows the deviation for 60 min evaluation time. In this case, the deviation is significantly higher and might even excess 10 %.

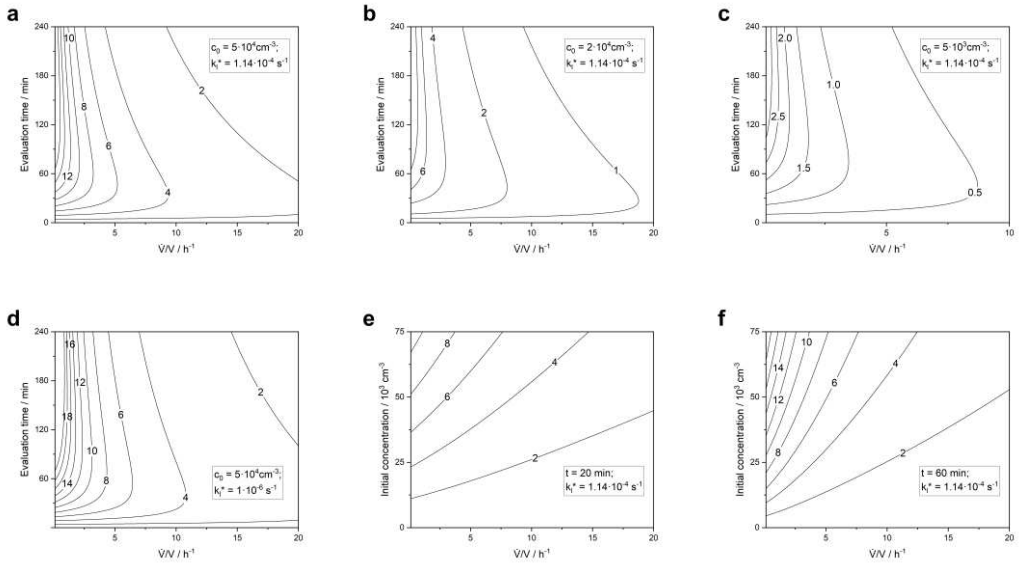

Figure 13. Calculated relative deviation *D* in % for determination of CADR by 'standard procedure' (equations 18/19/21) for $k_a = 3.46 \cdot \frac{10^{-9} cm^3}{s}$ and given parameters of k_l^*, c_0 and concentrations assessed for an evaluation time interval t with CADR determined by fitting to extended model (equation 11) as reference. High settling constant k_l^* (a-c & e-f) corresponds to conditions in the seminar room, low k_l^* (d) corresponds to community hall.

All deviations discussed above are due to different concentrations in experiments with and without air purifiers in operation. Therefore, a longer natural decay experiment with initial *and* final

 doi:10.20944/preprints202401.1858.v1

concentrations being identical with the respective decay experiment with air purifier, provides remedy. Simulations for all situations shown above revealed deviations less than 1 % in any case, if the natural decay is not determined for the same time interval but the same concentration ratio as the decay experiment with air purifiers.

4. Discussion

When measurements of aerosol dynamics in confined spaces are done using surrogate aerosol particles it is important to provide rather high concentrations in order to minimize errors by background aerosol sources. Measurements in different settings (large community hall and small seminar room) show that aggregation becomes relevant at least for concentrations exceeding 5,000 cm^{-3}. An extended model for the well-mixed case proves to be surprisingly well suited to describe the measured concentration course, at least for the community hall suggesting a well-mixed situation there. All relevant model parameters (source strength, CADR, kinetic coefficients for aggregation and linear decay mechanisms) were determined experimentally independently and were implemented into the extended model. This adjusted theoretical model describes the concentrations of surrogate aerosols pretty well.

For the seminar room, however, some small discrepancies can be detected which can be attributed to a lack of ideal mixing in this case. So, for well mixed enclosed spaces, the adequacy of the extended model is validated. It enables to better represent the curvature of concentration profiles at high particle concentrations (cf. also Figure 6 for comparison with the simple model), which are typical for surrogate aerosol experiments. This leads to a more accurate prediction of the steady state concentration. So, applying an extended model for surrogate aerosol experiments instead of the simple model is highly recommended at high particle concentrations.

It should be considered that linear decay coefficient k_l^* includes all effects which are proportional to the actual particle concentration. It is expected to depend on the surface to volume ratio, the geometry of the room (e.g. horizontal planes like tables which remove additional particles due to settling, all other surfaces), leakage flows and on particle size distribution. In contrast, the aggregation coefficient k_a should only depend on the particle size distribution, i.e. larger values for broader size distributions and in most cases slightly higher values also for smaller particles. Therefore, these constants must be determined depending on the particle source and the conditions in the respective room.

Besides the consideration of aerosol dynamics in indoor spaces, these findings have also implications for the determination of the CADR (clean air delivery rate) of air purifiers. They are typically examined in test chambers with surrogate aerosols as well. The standard procedure using linear fits of the logarithmic concentration decay with and without air purifiers in operation basically neglects the influence of the quadratic dependence of aggregation on concentration. In case of an evaluation time interval of 20 min and a maximum concentration of 20,000 cm^{-3} as proposed in e.g. the Chinese norm, the associated error might be considered minor. Nevertheless, for longer time intervals and higher concentrations this is not the case anymore. In these cases, it is advisable to use the presented extended model or to determine the natural decay for the identical concentration range as the overall decay rather than the identical evaluation time in order to avoid this error at all.

5. Conclusions

In the scope of this work, experiments were carried out observing particle concentrations by surrogate aerosols generated by an atomizer mimicking a steady particle emitter. It was shown that aerosols can spread rapidly in enclosed spaces when the room volume is well mixed. In only a few minutes, even a big community hall can depict an almost uniform aerosol concentration. This implies that the inhaled dose of aerosol particles is almost the same for all persons staying in the room independent of the distance to the emitter. People in very close distances in direction of exhaled air will face a slightly higher concentration about 1.5 to 2 times higher than the average at a distance of 2 m which is reasonable enough to consider this an adequate ‘safe distance’.

The approach of tracking particle concentrations by means of surrogate aerosols involves high particle concentrations and this study could show that the simple model with only the atomizer as particle source and air purifiers as particle sink does not represent concentration profiles at elevated concentrations above 5,000 particles per cm^3 in good approximation. For a more precise model description of the concentration profiles, additional effects such as sedimentation and aggregation need to be considered. For both effects, kinetic coefficients were determined from independent measurements and inserted into the model to obtain a more representative theoretical description of experimental data. Additionally, the atomizer's particle generation rate as well as the CADR of the applied air purifiers were determined experimentally by fitting the respective parameter in the derived model equation.

In case of CADR determination, it was shown that the CADR is below the manufacturer's specification although brand-new devices were used. Furthermore, some influence of bypass flows could be shown if the air purifiers are operated in close proximity.

Overall, all relevant model parameters (source strength, kinetic coefficients for sedimentation and aggregation, and CADRs) were determined independently and their insertion into an extended model leads to an accurate representation of the long-term concentration profiles and steady state concentrations.

The effect of aggregation causes a deviation of the concentration from an exponential decay, since it is proportional to the actual concentration squared. Therefore, it is shown that standard evaluation procedures for CADR do not cover this effect adequately. The resulting deviation causes a systematic underestimation of the CADR and this effect is increasing for lower air exchange rates, higher initial concentrations and longer evaluation time intervals. While for conditions as proposed in the norms the deviation is typically below 5 % it might become significantly larger and highly relevant if conditions are present which are more likely to apply to surrogate aerosol measurements in indoor spaces. However, these errors can be avoided by using the proposed extended model or by determining natural decay rates for identical concentration ratios compared to the decay with air purifiers instead of applying the identical evaluation time intervals.

In order to transfer experiments with surrogate aerosol particles to spreading of virus-laden respiratory aerosols, it is important to note, that they do not behave identical. Particularly, aggregation is relevant for surrogate aerosols (at least if concentrations above 5,000 particles per cm^3 are applied) but not for respiratory aerosols, since for the latter typical particle concentrations are way below this. Linear decay mechanisms however, are relevant for both types of aerosols. In order to have comparable values for k_l^* in both cases it is very important that the size distributions of surrogate and respiratory particle sizes are as similar as possible. In order to predict infection risks, the concentrations of contagious viruses must be calculated based on the approach presented in this paper. Experiments with surrogate aerosols allow the determination of k_l^*. The source strength must be assumed depending on the number of infected people and their activities. Furthermore, an additional decay mechanism has to be added to account for natural airborne virus deactivation [57]. Since this deactivation rate is also proportional to the number of active pathogens, the deactivation rate constant can just be added to k_l^*. All in all, the presented extended model can be taken for deductions of virus-laden respiratory aerosols if the corresponding adaptions of the parameters obtained from the surrogate aerosol experiments are considered.

Supplementary Materials: The following supporting information can be downloaded at the website of this paper posted on Preprints.org, Figure S1: title; Table S1: title; Video S1: title.

Author Contributions from Janis Beimdiek (JB) and Hans-Joachim Schmid (HJS): Conceptualization, HJS and JB; methodology, HJS and JB; validation, JB and HJS; formal analysis, HJS and JB; investigation, JB and HJS; resources, HJS; data curation, JB; writing—original draft preparation, JB; writing—review and editing, HJS; visualization, JB; supervision, HJS; project administration, JB and HJS. All authors have read and agreed to the published version of the manuscript.

Funding: This research received no external funding.

Data Availability Statement: All data presented in this study are available on request from the corresponding author.

Acknowledgments: The authors gratefully acknowledge valuable discussions on interpretation and calibration of CPC data with Dr. Carsten Kykal from TSI Incorporated. The support by TSI in providing some of the CPC devices is gratefully acknowledged. Moreover, we would like to thank the Freie Evangelische Gemeinde Paderborn for providing access to the community hall and the air purifiers.

Conflicts of Interest: The authors declare no conflict of interest.

References

1. Zhu, N.; Zhang, D.; Wang, W.; Li, X.; Yang, B.; Song, J.; Zhao, X.; Huang, B.; Shi, W.; Lu, R.; et al. A Novel Coronavirus from Patients with Pneumonia in China, 2019. *The New England journal of medicine* **2020**, *382*, 727–733, doi:10.1056/NEJMoa2001017.
2. Laue, M.; Kauter, A.; Hoffmann, T.; Möller, L.; Michel, J.; Nitsche, A. Morphometry of SARS-CoV and SARS-CoV-2 particles in ultrathin plastic sections of infected Vero cell cultures. *Sci. Rep.* **2021**, *11*, 3515, doi:10.1038/s41598-021-82852-7.
3. Scheuch, G. Breathing Is Enough: For the Spread of Influenza Virus and SARS-CoV-2 by Breathing Only. *Journal of aerosol medicine and pulmonary drug delivery* **2020**, *33*, 230–234, doi:10.1089/jamp.2020.1616.
4. Asadi, S.; Wexler, A.S.; Cappa, C.D.; Barreda, S.; Bouvier, N.M.; Ristenpart, W.D. Aerosol emission and superemission during human speech increase with voice loudness. *Sci Rep* **2019**, *9*, 2348, doi:10.1038/s41598-019-38808-z.
5. Han, Z.Y.; Weng, W.G.; Huang, Q.Y. Characterizations of particle size distribution of the droplets exhaled by sneeze. *Journal of the Royal Society, Interface* **2013**, *10*, 20130560, doi:10.1098/rsif.2013.0560.
6. Hartmann, A.; Lange, J.; Rotheudt, H.; Kriegel, M. Emissionsrate und Partikelgröße von Bioaerosolen beim Atmen, Sprechen und Husten, 2020.
7. Haslbeck, K.; Schwarz, K.; Hohlfeld, J.M.; Seume, J.R.; Koch, W. Submicron droplet formation in the human lung. *Journal of Aerosol Science* **2010**, *41*, 429–438, doi:10.1016/j.jaerosci.2010.02.010.
8. Papineni, R.S.; Rosenthal, F.S. The size distribution of droplets in the exhaled breath of healthy human subjects. *Journal of aerosol medicine : the official journal of the International Society for Aerosols in Medicine* **1997**, *10*, 105–116, doi:10.1089/jam.1997.10.105.
9. Schwarz, K.; Biller, H.; Windt, H.; Koch, W.; Hohlfeld, J.M. Characterization of exhaled particles from the healthy human lung--a systematic analysis in relation to pulmonary function variables. *Journal of aerosol medicine and pulmonary drug delivery* **2010**, *23*, 371–379, doi:10.1089/jamp.2009.0809.
10. Xie, X.; Li, Y.; Sun, H.; Liu, L. Exhaled droplets due to talking and coughing. *Journal of the Royal Society, Interface* **2009**, *6 Suppl 6*, S703-14, doi:10.1098/rsif.2009.0388.focus.
11. Xie, X.; Li, Y.; Chwang, A.T.Y.; Ho, P.L.; Seto, W.H. How far droplets can move in indoor environments--revisiting the Wells evaporation-falling curve. *Indoor Air* **2007**, *17*, 211–225, doi:10.1111/j.1600-0668.2007.00469.x.
12. GAeF. Position paper on aerosols and SARS-CoV-2. Available online: https://www.info.gaef.de/position-paper (accessed on 23 November 2023).
13. Smither, S.J.; Eastaugh, L.S.; Findlay, J.S.; Lever, M.S. Experimental aerosol survival of SARS-CoV-2 in artificial saliva and tissue culture media at medium and high humidity. *Emerging Microbes & Infections* **2020**, *9*, 1415–1417, doi:10.1080/22221751.2020.1777906.
14. van Doremalen, N.; Bushmaker, T.; Morris, D.H.; Holbrook, M.G.; Gamble, A.; Williamson, B.N.; Tamin, A.; Harcourt, J.L.; Thornburg, N.J.; Gerber, S.I.; et al. Aerosol and Surface Stability of SARS-CoV-2 as Compared with SARS-CoV-1. *The New England journal of medicine* **2020**, *382*, 1564–1567, doi:10.1056/NEJMc2004973.
15. Zhang, R.; Li, Y.; Zhang, A.L.; Wang, Y.; Molina, M.J. Identifying airborne transmission as the dominant route for the spread of COVID-19. *Proc. Natl. Acad. Sci. U. S. A.* **2020**, *117*, 14857–14863, doi:10.1073/pnas.2009637117.
16. Wang, C.C.; Prather, K.A.; Sznitman, J.; Jimenez, J.L.; Lakdawala, S.S.; Tufekci, Z.; Marr, L.C. Airborne transmission of respiratory viruses. *Science* **2021**, *373*, doi:10.1126/science.abd9149.
17. Morawska, L.; Cao, J. Airborne transmission of SARS-CoV-2: The world should face the reality. *Environment International* **2020**, *139*, 105730, doi:10.1016/j.envint.2020.105730.
18. Coronavirus disease (COVID-19): How is it transmitted? Available online: https://www.who.int/news-room/questions-and-answers/item/coronavirus-disease-covid-19-how-is-it-transmitted (accessed on 23 November 2023).
19. Adzic, F.; Roberts, B.M.; Hathway, E.A.; Kaur Matharu, R.; Ciric, L.; Wild, O.; Cook, M.; Malki-Epshtein, L. A post-occupancy study of ventilation effectiveness from high-resolution CO2 monitoring at live theatre events to mitigate airborne transmission of SARS-CoV-2. *Building and Environment* **2022**, *223*, 109392, doi:10.1016/j.buildenv.2022.109392.

20. Zhao, Y.; Gu, C.; Song, X. Evaluation of indoor environmental quality, personal cumulative exposure dose, and aerosol transmission risk levels inside urban buses in Dalian, China. *Environmental Science and Pollution Research International* **2023**, *30*, 55278–55297, doi:10.1007/s11356-023-26037-x.
21. Iwamura, N.; Tsutsumi, K. SARS-CoV-2 airborne infection probability estimated by using indoor carbon dioxide. *Environmental Science and Pollution Research International* **2023**, *30*, 79227–79240, doi:10.1007/s11356-023-27944-9.
22. Vassella, C.C.; Koch, J.; Henzi, A.; Jordan, A.; Waeber, R.; Iannaccone, R.; Charrière, R. From spontaneous to strategic natural window ventilation: Improving indoor air quality in Swiss schools. *International Journal of Hygiene and Environmental Health* **2021**, *234*, 113746, doi:10.1016/j.ijheh.2021.113746.
23. Kumar, P.; Rawat, N.; Tiwari, A. Micro-characteristics of a naturally ventilated classroom air quality under varying air purifier placements. *Environmental Research* **2023**, *217*, 114849, doi:10.1016/j.envres.2022.114849.
24. Alegría-Sala, A.; Clèries Tardío, E.; Casals, L.C.; Macarulla, M.; Salom, J. CO2 Concentrations and Thermal Comfort Analysis at Onsite and Online Educational Environments. *International Journal of Environmental Research and Public Health* **2022**, *19*, doi:10.3390/ijerph192316039.
25. Di Gilio, A.; Palmisani, J.; Pulimeno, M.; Cerino, F.; Cacace, M.; Miani, A.; Gennaro, G. de. CO2 concentration monitoring inside educational buildings as a strategic tool to reduce the risk of Sars-CoV-2 airborne transmission. *Environmental Research* **2021**, *202*, 111560, doi:10.1016/j.envres.2021.111560.
26. Rudnick, S.N.; Milton, D.K. Risk of indoor airborne infection transmission estimated from carbon dioxide concentration. *Indoor Air* **2003**, *13*, 237–245, doi:10.1034/j.1600-0668.2003.00189.x.
27. Peng, Z.; Jimenez, J.L. Exhaled CO2 as a COVID-19 Infection Risk Proxy for Different Indoor Environments and Activities. *Environmental Science & Technology Letters* **2021**, *8*, 392–397, doi:10.1021/acs.estlett.1c00183.
28. Bazant, M.Z.; Kodio, O.; Cohen, A.E.; Khan, K.; Gu, Z.; Bush, J.W. Monitoring carbon dioxide to quantify the risk of indoor airborne transmission of COVID-19. *Flow* **2021**, *1*, E10, doi:10.1017/flo.2021.10.
29. Schade, W.; Reimer, V.; Seipenbusch, M.; Willer, U. Experimental Investigation of Aerosol and CO2 Dispersion for Evaluation of COVID-19 Infection Risk in a Concert Hall. *International Journal of Environmental Research and Public Health* **2021**, *18*, 3037, doi:10.3390/ijerph18063037.
30. Duill, F.F.; Schulz, F.; Jain, A.; van Wachem, B.; Beyrau, F. Comparison of Portable and Large Mobile Air Cleaners for Use in Classrooms and the Effect of Increasing Filter Loading on Particle Number Concentration Reduction Efficiency. *Atmosphere* **2023**, *14*, 1437, doi:10.3390/atmos14091437.
31. Burgmann, S.; Janoske, U. Transmission and reduction of aerosols in classrooms using air purifier systems. *Phys. Fluids (1994)* **2021**, *33*, 33321, doi:10.1063/5.0044046.
32. Duill, F.F.; Schulz, F.; Jain, A.; Krieger, L.; van Wachem, B.; Beyrau, F. The Impact of Large Mobile Air Purifiers on Aerosol Concentration in Classrooms and the Reduction of Airborne Transmission of SARS-CoV-2. *International Journal of Environmental Research and Public Health* **2021**, *18*, 11523, doi:10.3390/ijerph182111523.
33. Szabadi, J.; Meyer, J.; Lehmann, M.; Dittler, A. Simultaneous temporal, spatial and size-resolved measurements of aerosol particles in closed indoor environments applying mobile filters in various use-cases. *Journal of Aerosol Science* **2022**, *160*, 105906, doi:10.1016/j.jaerosci.2021.105906.
34. Curtius, J.; Granzin, M.; Schrod, J. Testing mobile air purifiers in a school classroom: Reducing the airborne transmission risk for SARS-CoV-2. *Aerosol Science and Technology* **2021**, *55*, 586–599, doi:10.1080/02786826.2021.1877257.
35. Kähler, C.J.; Hain, R.; Fuchs, T. Assessment of Mobile Air Cleaners to Reduce the Concentration of Infectious Aerosol Particles Indoors. *Atmosphere* **2023**, *14*, 698, doi:10.3390/atmos14040698.
36. Kähler, C.J.; Fuchs, T.; Mutsch, B.; Hain, R. School education during the SARS-CoV-2 pandemic - Which concept is safe, feasible and environmentally sound? *medRxiv* **2020**, 2020.10.12.20211219, doi:10.1101/2020.10.12.20211219.
37. Küpper, M.; Asbach, C.; Schneiderwind, U.; Finger, H.; Spiegelhoff, D.; Schumacher, S. Testing of an Indoor Air Cleaner for Particulate Pollutants under Realistic Conditions in an Office Room. *Aerosol Air Qual. Res.* **2019**, *19*, 1655–1665, doi:10.4209/aaqr.2019.01.0029.
38. Dbouk, T.; Roger, F.; Drikakis, D. Reducing indoor virus transmission using air purifiers. *Phys. Fluids (1994)* **2021**, *33*, 103301, doi:10.1063/5.0064115.
39. Quintero, F.; Nagarajan, V.; Schumacher, S.; Todea, A.M.; Lindermann, J.; Asbach, C.; Luzzato, C.M.A.; Jilesen, J. Reducing Particle Exposure and SARS-CoV-2 Risk in Built Environments through Accurate Virtual Twins and Computational Fluid Dynamics. *Atmosphere* **2022**, *13*, 2032, doi:10.3390/atmos13122032.
40. Sabanskis, A.; Vidulejs, D.D.; Teličko, J.; Virbulis, J.; Jakovičs, A. Numerical Evaluation of the Efficiency of an Indoor Air Cleaner under Different Heating Conditions. *Atmosphere* **2023**, *14*, 1706, doi:10.3390/atmos14121706.
41. Srivastava, S.; Zhao, X.; Manay, A.; Chen, Q. Effective ventilation and air disinfection system for reducing coronavirus disease 2019 (COVID-19) infection risk in office buildings. *Sustainable Cities and Society* **2021**, *75*, 103408, doi:10.1016/j.scs.2021.103408.

42. Tobisch, A.; Springsklee, L.; Schäfer, L.-F.; Sussmann, N.; Lehmann, M.J.; Weis, F.; Zöllner, R.; Niessner, J. Reducing indoor particle exposure using mobile air purifiers-Experimental and numerical analysis. *AIP Adv.* **2021**, *11*, 125114, doi:10.1063/5.0064805.
43. Foster, A.; Kinzel, M. Estimating COVID-19 exposure in a classroom setting: A comparison between mathematical and numerical models. *Phys. Fluids (1994)* **2021**, *33*, 21904, doi:10.1063/5.0040755.
44. Gefahrstoffe. *GrdL* **2021**, *81*, doi:10.37544/0949-8036-2021-01-02.
45. Manoukian, A.; Quivet, E.; Temime-Roussel, B.; Nicolas, M.; Maupetit, F.; Wortham, H. Emission characteristics of air pollutants from incense and candle burning in indoor atmospheres. *Environ Sci Pollut Res* **2013**, *20*, 4659–4670, doi:10.1007/s11356-012-1394-y.
46. Bivolarova, M.; Ondráček, J.; Melikov, A.; Ždímal, V. A comparison between tracer gas and aerosol particles distribution indoors: The impact of ventilation rate, interaction of airflows, and presence of objects. *Indoor Air* **2017**, *27*, 1201–1212, doi:10.1111/ina.12388.
47. Chan, W.R.; Logue, J.M.; Wu, X.; Klepeis, N.E.; Fisk, W.J.; Noris, F.; Singer, B.C. Quantifying fine particle emission events from time-resolved measurements: Method description and application to 18 California low-income apartments. *Indoor Air* **2018**, *28*, 89–101, doi:10.1111/ina.12425.
48. *ANSI/AHAM AC-1-2020*: *Method for Measuring Performance of Portable Household Electric Room Air Cleaners;* American National Standards Institute (ANSI) / Association of Home Appliance Manufacturers (AHAM): Washington, DC, 2020.
49. *GB/T 18801-2015*: *Air cleaner;* Standardization Administration of the People's Republic of China: Beijing, 2015.
50. Burdack-Freitag, A.; Buschhaus, M.; Grün, G.; Hofbauer, W.K.; Johann, S.; Nagele-Renzl, A.M.; Schmohl, A.; Scherer, C.R. Particulate Matter versus Airborne Viruses—Distinctive Differences between Filtering and Inactivating Air Cleaning Technologies. *Atmosphere* **2022**, *13*, 1575, doi:10.3390/atmos13101575.
51. Schmohl, A.; Buschhaus, M.; Norrefeldt, V.; Johann, S.; Burdack-Freitag, A.; Scherer, C.R.; Vega Garcia, P.A.; Schwitalla, C. Incremental Evaluation Model for the Analysis of Indoor Air Measurements. *Atmosphere* **2022**, *13*, 1655, doi:10.3390/atmos13101655.
52. Nazaroff, W.W.; Cass, G.R. Mathematical modeling of indoor aerosol dynamics. *Environ. Sci. Technol.* **1989**, *23*, 157–166, doi:10.1021/es00179a003.
53. Nazaroff, W.W. Indoor particle dynamics. *Indoor Air* **2004**, *14 Suppl 7*, 175–183, doi:10.1111/j.1600-0668.2004.00286.x.
54. Nazaroff, W.W. Indoor bioaerosol dynamics. *Indoor Air* **2016**, *26*, 61–78, doi:10.1111/ina.12174.
55. Schumacher, S.; Banda Sanchez, A.; Caspari, A.; Staack, K.; Asbach, C. Testing Filter-Based Air Cleaners with Surrogate Particles for Viruses and Exhaled Droplets. *Atmosphere* **2022**, *13*, 1538, doi:10.3390/atmos13101538.
56. Lee, K.W.; Chen, H. Coagulation Rate of Polydisperse Particles. *Aerosol Science and Technology* **1984**, *3*, 327–334, doi:10.1080/02786828408959020.
57. Biryukov, J.; Boydston, J.A.; Dunning, R.A.; Yeager, J.J.; Wood, S.; Reese, A.L.; Ferris, A.; Miller, D.; Weaver, W.; Zeitouni, N.E.; et al. Increasing Temperature and Relative Humidity Accelerates Inactivation of SARS-CoV-2 on Surfaces. *mSphere* **2020**, *5*, doi:10.1128/mSphere.00441-20.